Available online at www.sciencedirect.com

SCIENCE DIRECT®

ELSEVIER

Carbohydrate Research 340 (2005) 1529–1537

Carbohydrate
RESEARCH

# Solid-state phase behaviour of dodecylglycosides

Caroline A. Ericsson,[a] Louise C. Ericsson[a] and Stefan Ulvenlund[a,b,*]

[a]*Department of Physical Chemistry 1, Centre of Chemistry and Chemical Engineering, Lund University, PO Box 124, S-221 00 Lund, Sweden*
[b]*AstraZeneca R&D Lund, S-221 87 Lund, Sweden*

Received 5 March 2005; accepted 31 March 2005

---

**Abstract**—The solid-state phase behaviour of lyophilised *n*-dodecyl-β-D-glucoside (β-$C_{12}G_1$), *n*-dodecyl-β-D-maltoside (β-$C_{12}G_2$) and *n*-dodecyl-β-D-maltotrioside (β-$C_{12}G_3$) has been investigated by differential scanning calorimetry (DSC) and X-ray techniques. For β-$C_{12}G_1$, lyophilisation results in a formation of a crystalline anhydrate. The lamellar spacing (37 Å) is consistent with an alkyl chain packing in which the chains are not interdigitated. At 80 °C, the material melts into a lamellar liquid crystal with a lamellar spacing of 32 Å, which suggests that the non-interdigitated chain packing of the crystalline state is retained in the liquid crystal. In contrast, lyophilisation of β-$C_{12}G_2$ and β-$C_{12}G_3$ results in the formation of a glassy state, best described as a frozen version of the lamellar liquid crystal. For β-$C_{12}G_2$, the lamellar spacing in the glass and liquid crystal suggests interdigitation of the alkyl chains. The glass transition temperature was found to be 65 °C for β-$C_{12}G_2$ and 100 °C for β-$C_{12}G_3$, which compares favourably with the glass transition of the parent carbohydrates. A second crystalline modification of β-$C_{12}G_1$ was prepared by precipitation from an aqueous solution at temperatures below the Krafft point (38 °C). For this modification, the lamellar distance (24 Å) is consistent with interdigitated alkyl chains. At 50 °C, the crystalline material melts into a liquid crystalline phase. The material also readily loses water and rapidly re-crystallises to the anhydrate. The amount of water lost upon drying is consistent with the idea that the material is a monohydrate of β-$C_{12}G_1$. The drying and re-crystallisation processes give rise to 'pre-transitions' in the DSC thermograms and illustrate the importance of careful control of water in any analysis of the phase behaviour of alkylglycosides.

*Keywords:* Alkylglycosides; DSC; X-ray diffraction; Hydrate

---

## 1. Introduction

In contrast to most other surfactant systems, the head-groups of sugar-based surfactants interact strongly with each other. This interaction stems from intermolecular hydrogen bonds between hydroxyl groups in the sugar moieties and makes sugar-based surfactants very interesting in terms of their solid phase behaviour.

In alkylglycosides, the sugar unit and the alkyl chain are linked via a glycoside bond. Alkylglycosides are of particular relevance for 'green' industrial applications, since they are stable against hydrolysis, yet readily biodegradable. Previous investigations of the thermotropic behaviour of alkylglycoside surfactants have established that they demonstrate so-called 'double melting points'.[1–8] The two melting points are conventionally referred to as the *chain melting* and the *clearing point*. They are generally widely separated in temperature, and a liquid crystalline phase prevails at intermediate temperatures. The existence of this phase is possible to attribute to the strong attractive interactions between adjacent head-groups.[5]

Besides the two main melting points of alkylglycosides, one or two pre-transitions are often observed in DSC thermograms. The origin of these pre-transitions is less well understood. However, a number of studies suggest that pre-transitions are not observed in systems that have been carefully dried prior to measurement.[8] Based on this observation and other supplementary evidence, Kocherbitov and Söderman have suggested the

---

[*] Corresponding author. Tel.: +46 46 337847; fax: +46 46 337128; e-mail: stefan.ulvenlund@astrazeneca.com

0008-6215/$ - see front matter © 2005 Elsevier Ltd. All rights reserved.
doi:10.1016/j.carres.2005.03.015

pre-transition observed for *n*-octyl-α-D-glucoside ($\alpha C_8G_1$) to be a crossing of the peritectic point.[8]

The understanding of the structure of crystalline and liquid crystalline phases of alkylglycosides is still sketchy. For the β-alkylglucosides, no single-crystal X-ray data are available and the discussion of their crystal structure has to be based on single-crystal data on the corresponding α-anomers. However, the strong impact of intermolecular head-group interaction on phase structure and behaviour makes direct comparison of the α- and β-anomers difficult. In crystalline α-alkylglucosides the bilayer is composed of interdigitated alkyl chains sandwiched between head-groups connected in a hydrogen-bonded network.[9] It has been claimed that the crystalline β-glucosides differ from the α-analogues in the sense that they are hydrated due to a 'less perfect packing' of the head-groups,[10] and that their chains are not interdigitated.[11] The latter claim is based on the observation that the inter-lamellar spacing of the β-anomers is often larger than that of the corresponding α-anomers.[5,10–12] However, contradictory conclusions can also be found in the literature.[13] It is reasonable to assume that the ambiguities in the literature, at least in part, are due to the fact that the hydrates of alkylglycosides readily lose their water of crystallisation several degrees below the melting for the anhydrous material.[11] Consequently, more detailed studies of the effects of water of crystallisation on the phase structure and phase behaviour are called for.

The properties of the non-crystalline solid state of alkylglycosides represent another interesting area of research. Recent results from X-ray techniques and calorimetry have shown that anhydrous *n*-octyl- and *n*-decyl-β-D-maltoside ($\beta$-$C_8G_2$ and $\beta$-$C_{10}G_2$) form glasses at room temperature.[14] These glasses may be regarded as 'frozen' versions of a lamellar liquid crystalline phase. In contrast, the non-crystalline state of anhydrous long-chain maltosides $\beta$-$C_{14}G_2$ and $\beta$-$C_{16}G_2$ is best described as gel phases, in which the alkyl chains are ordered in a hexagonal array, whereas the head-groups are disordered ('glassy').[27] For glucosides, no glass transition is observed, which has been explained by the lower number of intermolecular hydrogen bonds in these systems.[14] Consequently, we again find that interactions between head-groups are decisive for the solid-state behaviour of alkylglycosides.

In the present study, *n*-dodecyl-β-D-glucoside ($\beta$-$C_{12}G_1$) has been thoroughly investigated in order to confirm and extend previous studies of the solid-state phase behaviour of alkylglucosides.

Previous investigations on the solid-state phase behaviour of $\beta$-$C_{12}G_1$ show the material to display the characteristic double melting points at ca. 80 and 143 °C.[3,4,15–17] Additional transitions (referred to as 'pre-transitions' or 'solid–solid transitions') have been observed at 52–63 °C.[16,17] However, these transitions have not been investigated in any detail and their relation to phase structure and possible loss of water of crystallisation has not been elucidated. Therefore, the present study uses a combination of X-ray techniques and calorimetry in order to correlate phase behaviour with phase structure in systems where the amount of water is rigorously controlled.

A second objective of the present study is to extend our understanding of the non-crystalline state of alkylglycosides by investigating the effect of head-group size on phase behaviour. To this end, the properties of lyophilised (freeze-dried) $\beta$-$C_{12}G_1$ have been compared with those of *n*-dodecyl-β-D-maltoside ($\beta$-$C_{12}G_2$) and *n*-dodecyl-β-D-maltotrioside ($\beta$-$C_{12}G_3$).

## 2. Experimental

### 2.1. Materials and sample preparation

*n*-Dodecyl-β-D-glucoside ($\beta$-$C_{12}G_1$), *n*-dodecyl-β-D-maltoside ($\beta$-$C_{12}G_2$) and *n*-dodecyl-β-D-maltotrioside ($\beta$-$C_{12}G_3$) were purchased from Anatrace Inc. (Maumee, OH) and were of ANAGRADE™ quality. The supplier states a purity of >97% for all three compounds.

Water was distilled and further purified on a Purelab Plus apparatus, equipped with a final filter with a pore size of 0.1 μm. *tert*-Butanol was obtained from Acros organics (New Jersey, USA) and had a purity of 99.5%.

Freeze-drying was preformed on a Christ Alpha freeze-drier. The powders were completely dissolved in *tert*-butanol at room temperature in round bottom flasks. The solutions were rapidly quenched on an isopropanol/dry ice bath while constantly rotating the flask. Drying was performed under vacuum (<0.5 mbar) for at least 24 h.

Re-crystallisation of $\beta$-$C_{12}G_1$ from water was achieved by dissolving the starting material at 45 °C. The system was left to equilibrate at room temperature for 2 days, which ensured quantitative precipitation. The precipitate was isolated from the supernatant by means of centrifugation and subsequently dried at room temperature under vacuum for at least 48 h.

### 2.2. Solid-state differential scanning calorimetry (SS-DSC)

Solid-state DSC was preformed on a TA Instrument Q1000 equipped with a modulation option. A typical experiment was carried out with a modulation of ±0.5 °C every 40 s with an underlying heating rate of 2.5 °C/min. The heating rate was in a heat-only mode, that is, the overlaid temperature was always positive. The cell was purged with dry nitrogen at an average rate of 50 mL/min.

The presence of water (which may be retained bulk water and/or water of crystallisation) obviously has a major impact on the phase behaviour of solid materials and therefore on their DSC characteristics. For this reason, SS-DSC analysis of a given material was generally conducted according to both of the following protocols.

1. Experiments with the sample enclosed in *sealed* aluminium pans, which allows for measurements in which the water content is constant.
2. Experiments with the sample enclosed in aluminium pans with a loosely fitted lid, which allows for any released water to escape from the sample during heating. These pans will henceforth be referred to as '*open*'. The walls of the open pans are somewhat thinner than those in the sealed ones, which increase the sensitivity of the measurement. After ensuring that no thermal events occurred below 30 °C, experiments with open pans were started by drying the sample in the pan for 60 min at 30 °C under a flow of dry nitrogen. It then continued with a heat ramp up to a final temperature.

As described in detail elsewhere,[18] modulating DSC makes it possible to separate the total heat flow (d*Q*/d*t*) into a heat-rate dependent component (the so-called *reversing* heat flow) and a kinetic (temperature and time dependent) component, denoted as *non-reversing* heat flow. This separation of components makes it possible to analyse thermal events in greater detail than in conventional DSC. In particular, the identification of glass transitions is vastly facilitated.

Temperatures reported in this work for endothermic (exothermic) events are the maximum (minimum) of the corresponding peak in the thermogram. Glass transition temperatures are defined as the mid-point of the corresponding step-change in $C_P$ (reversing heat flow).

### 2.3. Thermogravimetric analysis (TGA)

TGA experiments were performed on a TA Instrument Q500 thermogravimetric analyser. Measurements were performed according to two different, but complementary protocols. In the first protocol, the material under study was dried in the sample compartment at 30 °C for 60 min under a flow of dry nitrogen. The sample was then heated at 5 °C/min from 30 to 200 °C. In the second protocol, the drying step was omitted and the heat ramp started directly after the sample had been placed in the sample compartment. During the measurement and the initial drying step (if applicable), the sample compartment was flushed with dry nitrogen at a rate of 60 mL/min.

### 2.4. Liquid differential scanning calorimetry

A MCS DSC instrument from Microcal Inc. (Northampton, MA) was used for DSC studies of liquid samples. The sample cell volume was 1.16 cm$^{-3}$. β-$C_{12}G_1$ was dissolved in water to a concentration of 0.1 wt % at elevated temperature and then equilibrated at room temperature until a precipitate formed. Before DSC measurement, the samples were homogenised on a vortex stirrer and de-aerated under vacuum for half an hour. The sample was injected to the sample cell and scanned at a rate of 60 °C/h in the temperature interval 11–60 °C.

### 2.5. Powder X-ray diffraction (PXRD)

All X-ray diffraction experiments conducted at room temperature were performed on a Scintag XDS 2000 $\theta$–$\theta$ diffractometer (Scintag Inc., USA), whereas experiments at elevated temperatures were performed on a Panalytical X'Pert Pro. The Scintag diffractometer was equipped with a liquid-nitrogen-cooled solid-state germanium detector and spinning sample holders. The sample holders consisted of open Teflon cups. Measurements were performed over an angular range of 2–35° (2$\theta$), using Cu$K_\alpha$ radiation (1.5418 Å, 45 kV and 30 mA). A continuous scan rate of 1°/min and a step size of 0.03° were used. On the primary side, 2- and 4-mm slits were used, whereas the secondary side used 0.5- and 0.3-mm slits.

PXRD experiments at elevated temperatures were performed on a Panalytical X'Pert Pro $\theta$–$\theta$ diffractometer equipped with an X'Celerator detector. Measurements were conducted with an increasing temperature of 1 °C/min, a continuous scan rate of 6.1°/min and a step size of 0.017°. The angular range was 2–40° (2$\theta$) and the radiation was Cu$K_\alpha$ (1.5418 Å, 45 kV and 40 mA). Samples were contained in a cavity in a metal plate and measurements were performed without spinning the sample holder.

### 2.6. Small- and wide-angle X-ray scattering (SAXS and WAXS)

A Kratky compact small-angle system with linear collimation and a position sensitive detector was used in the SAXS and WAXS experiments. Measurements were performed between 25 and 130 °C using Cu$K_\alpha$ radiation (1.5418 Å). SAXS and WAXS data were recorded simultaneously. The sample cell was equipped with mica windows and sealed with rubber O-rings.

## 3. Results and discussion

### 3.1. Lyophilised β-$C_{12}G_1$, β-$C_{12}G_2$ and β-$C_{12}G_3$ freeze-dried from *tert*-butanol

Freeze-drying of β-$C_{12}G_1$ from *tert*-butanol produces an extremely fluffy solid material. Considering that freeze-drying often produces non-crystalline materials, it is noteworthy that PXRD and WAXS in this case provide diffractograms comprising well-defined Bragg reflections (Fig. 1). This observation, together with the mode of preparation, strongly suggests that the material is a crystalline anhydrate. The data also show that this modification of β-$C_{12}G_1$ has an inter-lamellar spacing of 37 Å (Table 1). The lamellar distance of β-$C_{12}G_1$ in the crystalline state may be estimated by extrapolation of data on shorter-chain homologues with non-interdigitated chains reported by Hoffman et al.[11] This estimate yields a distance of 39 Å for β-$C_{12}G_1$, in fair agreement with our experimental results.

The thermogram of the material displays only two events, namely endothermic peaks at 79 and 142 °C (Table 2), which agrees with the literature data.[4,15] Thermograms recorded in sealed and open pans were found to be identical, which provides further support for the assignment of the material as anhydrous. Furthermore, the thermogram does not provide any evidence for any solid-state transitions, that is, there is no evidence of any polymorphism.

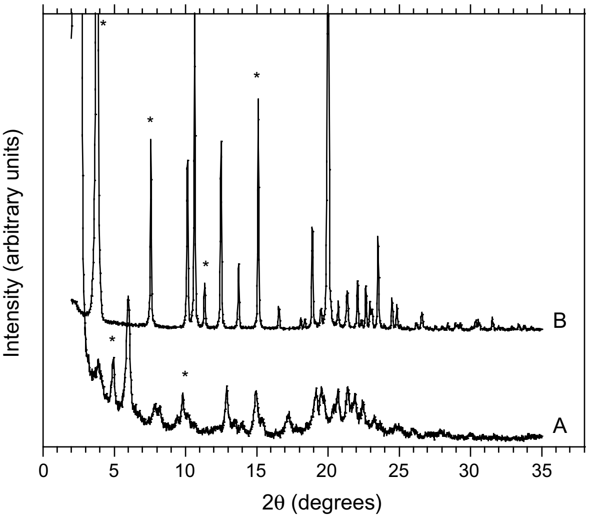

**Figure 1.** Powder X-ray diffractograms at 25 °C for (A) freeze-dried β-$C_{12}G_1$ from *tert*-butanol and (B) precipitate of β-$C_{12}G_1$ formed from water at room temperature. The peaks corresponding to inter-lamellar reflections are marked with asterisks.

**Table 1.** SAXS data for the different solid forms of β-$C_{12}G_1$

| Temperature (°C) | Precipitate from $H_2O$ at rt (hydrate) | Freeze-dried from *tert*-butanol (anhydrate) |
|---|---|---|
| 25 | 29, **25**, 24 *C* | 37 *C* |
| 55 | 53, 47, 41, **38** *C* | 37 *C* |
| 75 | 53, 47, 41, **38** *C* | 37 *C* |
| 95 | 32 | 32 |
| 115 | 31 | 31 |
| 135 | 30 | 30 |

In each entry, the inter-lamellar spacing *d* is given in units of Å. *C* denotes crystallinity (as determined from WAXS data). Distances marked in **bold** type correspond to peaks that are distinctly more intense in the diffractogram than the other peaks. Bold lines between two temperatures denote that a DSC transition is observed between these temperatures under conditions where water can escape during the experiment (see also Table 2).

When passing the endothermic peak at 79 °C, the high-angle Bragg reflections are lost and only a broad peak centred at 20° (ca. 4.4 Å) is observed. This observation makes it possible to assign this peak as an order–disorder transition, and thus as a transition from a crystalline phase to a lamellar liquid crystal phase (a 'chain melting'). The SAXS data reveals that the lamellar distance decreases to 32 Å during the order–disorder transition (Table 1), which is fairly consistent with the general observation that the effective length of an alkyl chain is reduced by approximately 20% in a liquid crystalline phase, as compared to a crystalline one.[19] The data thus suggest that the non-interdigitated state of the alkyl chains is retained in the liquid crystal. The lamellar distance decreases from 32 to 30 Å, when the temperature is increased up to 135 °C (Table 1). This inverse dependence of lamellar spacing on temperature again agrees with what is normally observed for liquid crystals.[20] When passing the second DSC peak at 143 °C, all small- and wide-angle X-ray reflections are lost, which shows this event to correspond to the clearing point, where an isotropic melt is formed.

In order to investigate the physical stability of freeze-dried β-$C_{12}G_1$, it was kept at room temperature for 4 months in a sealed container and then re-analysed by SS-DSC. The thermogram showed no differences as compared with that recorded directly after freeze-drying, and the material can be concluded to be stabile at room temperature for quite a substantial time.

In contrast to β-$C_{12}G_1$, β-$C_{12}G_2$ and β-$C_{12}G_3$ freeze-dried from *tert*-butanol display PXRD diffractograms that are devoid of Bragg reflections (Fig. 2). Rather, the diffractograms contain only a broad peak centred around 20° (ca. 4.4 Å). These characteristics are consistent with what is normally observed for molten hydrocarbon chains in lamellar liquid crystals.[19] However, DSC thermograms comprise a well-defined glass transition in both cases (Fig. 3) and therefore clearly show that the materials are to be regarded as glasses, rather than super-cooled liquid crystalline phases, at room temperature. The data also show that an increase of the head-group length by one glucose unit results in an increase of the glass transition, from 65 °C for β-$C_{12}G_2$ to ~100 °C for β-$C_{12}G_3$. This increase is presumably attributable to more thermal energy being required to transform the glass to a liquid crystalline phase when the number of intermolecular hydrogen bonds between head-groups increases. SAXS data for β-$C_{12}G_2$ at room temperature show a single reflection at 39 Å. Above the glass transition temperature, the distance decreases to

**Table 2.** Transition temperatures $T$ and enthalpy changes $\Delta H$, as obtained by DSC for β-$C_{12}G_1$

| Sample | Transition temperature (°C) | $\Delta H$ (kJ mol$^{-1}$) | Assignment |
|---|---|---|---|
| *Data recorded using open pans* | | | |
| Freeze-dried from *tert*-butanol | 79.1 | 24.7 | Chain melting |
| | 142.2 | 1.4 | Clearing point |
| Freeze-dried from *tert*-butanol stored at rt for 2 weeks | 79.0 | 24.1 | Chain melting |
| | 142.1 | 1.2 | Clearing point |
| Precipitate from water—first heating scan | 49.4 | 17.3 | Solid–solid |
| | 80.6 | 19.9 | Chain melting |
| | 143.4 | 1.1 | Clearing point |
| Precipitate from water—first cooling scan | 142.6 | −1.3 | Maltese cross |
| | 46.9 | −13.5 | Crystallisation |
| Precipitate from water—second heating scan | ~40 | — | Crystallisation? |
| | 80.3 | 22.7 | Chain melting |
| | 143.4 | 1.1 | Clearing point |
| Precipitate from water stored in oven at 55 °C for 65 h | 81.1 | 25.4 | Chain melting |
| | 143.4 | 1.3 | Clearing point |
| *Data recorded using sealed pans* | | | |
| Freeze-dried from *tert*-butanol | 79.2 | 24.4 | Chain melting |
| | 142.4 | 1.4 | Clearing point |
| Precipitate from water—first heating scan | 49.5 | 53.6 | Chain melting |
| | 144.0 | 1.4 | Clearing point |
| Precipitate from water—first cooling scan | 143.7 | 1.1 | Maltese cross |
| | ~40 | — | Crystallisation? |
| Precipitate from water—second heating scan | 42.4 | −13.0 | Crystallisation |
| | 79.8 | 25.1 | Chain melting |
| | 144.0 | 1.4 | Clearing point |

The transition temperature is defined as the corresponding maximum in the total heat flow.

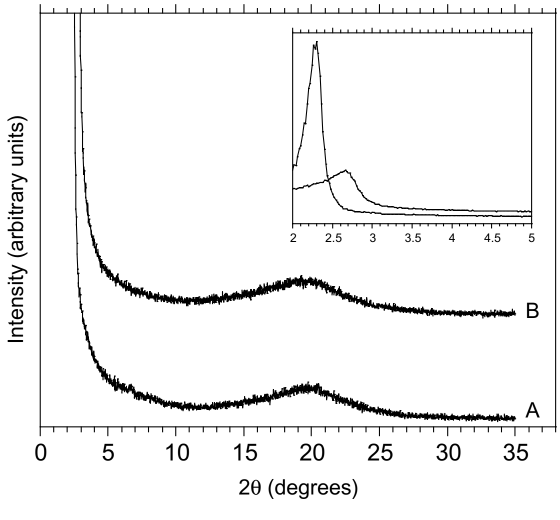

**Figure 2.** Powder X-ray diffractograms for (A) freeze-dried β-$C_{12}G_2$ and (B) freeze-dried β-$C_{12}G_3$. The insert shows an expansion of the small-angle region.

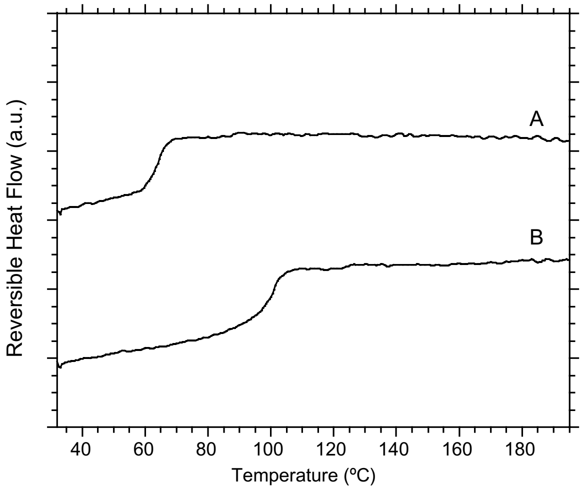

**Figure 3.** Reversing heat flow as measured with solid-state DSC for (A) freeze-dried β-$C_{12}G_2$ and (B) freeze-dried β-$C_{12}G_3$ from *tert*-butanol.

38 Å, but returns to 39 Å upon cooling to room temperature. Assuming an alkyl chain length of 16.7 Å and a head-group length of 12 Å,[21] the observed reflections are consistent with a lamellar structure in which the alkyl chains are interdigitated. The observation that the liquid crystal of β-$C_{12}G_2$ comprises interdigitated alkyl chains, whereas the chains in the liquid crystal of

β-$C_{12}G_1$ are non-interdigitated may be understood as an effect of the larger size of the maltose head-group. The diffractograms of β-$C_{12}G_3$ freeze-dried from *tert*-butanol comprise a low-angle peak that is very broad, which suggests that the molecules do not arrange themselves into a lamellar structure with a well-defined bilayer thickness (Fig. 2). In this case, the large size and inherent flexibility of the head-groups may be assumed to lead to substantial variation in bilayer thickness, which smears out the X-ray diffraction.

In addition to the glass transition, the DCS thermograms of freeze-dried β-$C_{12}G_2$ and β-$C_{12}G_3$ comprise an endothermic peak at elevated temperatures. This feature is observed at 244 °C for β-$C_{12}G_2$ and >250 °C for β-$C_{12}G_3$, and can be readily assigned as the clearing point. Our data on the clearing point of β-$C_{12}G_2$ is in agreement with the literature.[2,15,22] For β-$C_{12}G_3$, our data give a higher clearing point than previously reported (228 °C).[22]

Together with the X-ray data, the DSC results thus show that lyophilised β-$C_{12}G_2$ and β-$C_{12}G_3$ are to be regarded as glasses at room temperature. This makes it interesting to consider the glass transition temperatures of the parent carbohydrates. For maltose, the glass transition temperature is 73 °C, whereas that of maltotriose is 99 °C.[23] We therefore find evidence that the glass transition temperature of β-$C_{12}G_2$ and β-$C_{12}G_3$ is primarily governed by the nature of their head-groups, in agreement with the more general observation that the solid-state behaviour of alkylglycosides is dictated by head-group characteristics. However, the same conclusion is not directly applicable to β-$C_{12}G_1$. The glass transition temperature of glucose is 39 °C,[24] yet β-$C_{12}G_1$ forms a crystalline material, rather than a glass, upon lyophilisation.

### 3.2. Precipitate of β-$C_{12}G_1$ from water

β-$C_{12}G_1$ is practically insoluble in water at room temperature. However, previous studies show that at slightly higher temperatures (>38 °C), the β-$C_{12}G_1$/water system comprises a two-phase domain with two micellar phases in equilibrium.[25] The present work confirms these previous findings in the sense that the DSC thermogram for a 0.1 wt % β-$C_{12}G_1$ solution was found to show a single endothermic peak centred at 38 °C, corresponding to an enthalpy change of 33 kJ/mol. This point represents the phase transition from dispersed crystals to the two-phase micellar domain.

An aqueous solution of β-$C_{12}G_1$ heated to temperatures above 38 °C and then left to equilibrate at room temperature was found to produce a precipitate. The PXRD diffractogram of the precipitate at room temperature displays a crystalline pattern with relatively few, but very strong Bragg peaks (Fig. 1). The diffractogram comprises first through fourth order inter-lamellar reflections corresponding to a spacing of 23.4 Å. The diffractogram also shows that the material does not contain detectable amounts of the crystalline anhydrate obtained by freeze-drying from *tert*-butanol. Considering the high scattering efficiency, the relatively low number of Bragg peaks, the presence of one and only one set of inter-lamellar reflections and the perfectly flat base line, the PXRD data strongly suggest that the material is not only highly crystalline, but also that it comprises only one crystalline modification and contains very little, if any, amorphous material. It is therefore surprising that the SAXS diffractogram comprises more than one set of reflections (Table 1). However, the reflections are centred at ca. 25 Å.

TGA experiments were conducted on the precipitate in order to establish its water content. When the precipitate was analysed without any initial drying step, a weight loss of 4.5 wt % was found to take place between 25 and 55 °C, whereas the weight remained constant at higher temperatures (Fig. 4). On the other hand, if the material was analysed with initial drying at 30 °C for 60 min, the initial drying resulted in a weight loss of 4 wt %, whereas the subsequent temperature increase was found to result in a further loss of 0.5 wt %. Regardless of experimental protocol, the total weight loss was thus found to equal 4.5 wt %. The calculated water content of β-$C_{12}G_1 \cdot H_2O$ is 4.9 wt %. The idea that water of crystallisation is lost even under the mild conditions employed in the TGA experiments is fully consistent with previous data on alkylglycosides.[11] TGA and PXRD data are therefore consistent with the idea that the dominating crystalline modification in the precipitate is a monohydrate of β-$C_{12}G_1$. It is possible that the occurrence of more than one set of reflections in SAXS is an artefact caused by a loss of water during measurement.

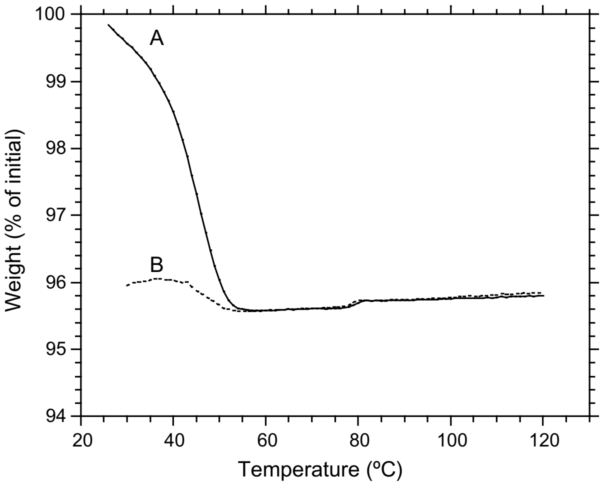

**Figure 4.** TGA analysis for precipitate of β-$C_{12}G_1$ formed from water. (A) measured without initial drying and (B) dried at 30 °C for 60 min prior to analysis.

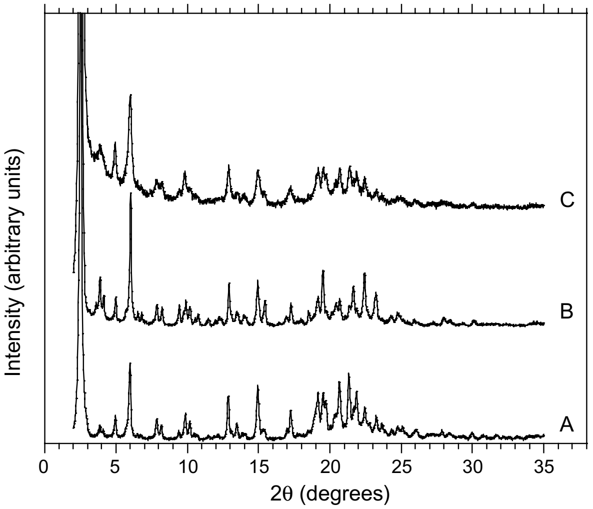

**Figure 5.** Powder X-ray diffractograms for β-$C_{12}G_1$ precipitate from water (A) dried at 40 °C for 2 weeks and then cooled to rt, (B) dried at 55 °C for 65 h and then cooled to rt and (C) freeze-dried from *tert*-butanol.

Drying of the precipitate under ambient atmosphere at temperatures in the range 40–55 °C, followed by cooling to room temperature was found to result in a formation of the crystalline anhydrate obtained also by freeze-drying from *tert*-butanol (Fig. 5). Consequently, we may conclude that the crystalline hydrate is prone to dehydration and subsequent re-crystallisation, even under comparably mild conditions. This makes further characterisation and data interpretation somewhat more challenging than is the case for the freeze-dried material. In particular, the credibility of data interpretation hinges on careful consideration of the question whether a given experiment is conducted under conditions where the water is retained during measurement, or not.

If the precipitate is subjected to solid-state DSC analysis in an open pan after initial drying at 30 °C, the thermogram comprises two peaks that are virtually identical to those of the material obtained by freeze-drying, namely those corresponding to the chain melting and the clearing point of the crystalline anhydrate (Table 2). However, the thermogram also contains an additional, markedly skew-symmetric endothermic peak at ca. 50 °C (Fig. 6, Table 2). This peak coincides with a transition reported in the literature, alternatively referred to as a 'solid–solid transition', 'loss of water' or a 'pre-transition'.[16,17] When the precipitate is analysed in a sealed pan, on the other hand, the thermogram contains a considerably more symmetric peak at 49 °C, whereas the transition at 80 °C is not observed (Fig. 6, Table 2). These observations seem to shed some light on the previous ambiguities in the literature. Our results strongly suggest that the transition at 49 °C corresponds to the melting of a crystalline hydrate into a hydrated liquid crystalline phase. However, if water is not carefully retained during measurement (as in experiments conducted in an open pan), the hydrated liquid crystalline phase very rapidly loses water and re-crystallises to the anhydrous modification, the chain melting of which produces the peak at 80 °C. The drying process may also be assumed to make the peak at ca. 50 °C skew-symmetric. The suggested behaviour of β-$C_{12}G_1$ therefore seems to provide a direct analogy to the behaviour of α-$C_8G_1$, for which Kocherbitov and Söderman have showed that a pre-transition is observed in the thermogram if, and only if, traces of water is present.[8]

Temperature-cycling DSC experiments provide additional information about the drying and re-crystallisation processes. Upon cooling after initial heating to 150 °C, DSC analysis of a sample in an open pan reveals two exothermic peaks, at 143 and 47 °C (Fig. 6, Table 2). In the subsequent heating scan, the melting point of the anhydrate at 80 °C is observed, whereas the endothermic peak at 50 °C has vanished. These observations are expected, based on the assumption that the 50 °C peak corresponds to drying and subsequent re-crystallisation of the hydrate. In this picture, the exothermic

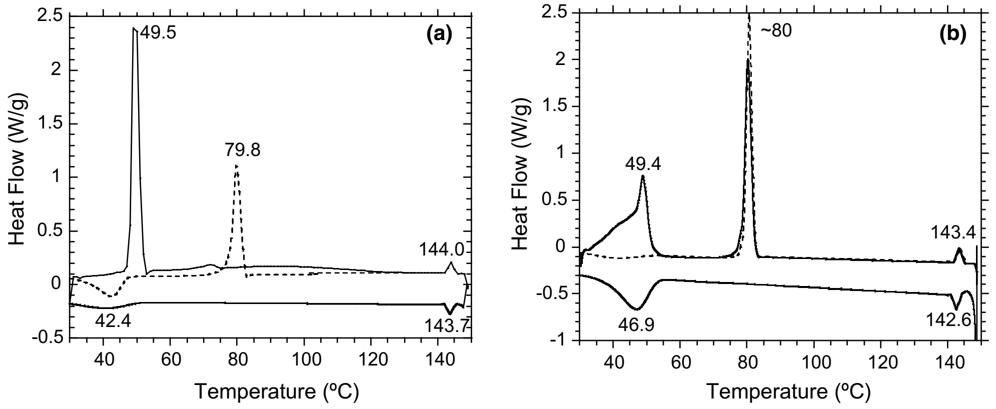

**Figure 6.** Temperature-cycling solid-state DSC thermograms of β-$C_{12}G_1$ precipitated from water where (a) were recorded in a sealed pan and (b) in an open pan. The second heating scan is denoted with a dotted trace.

peak at 47 °C is the crystallisation of the anhydrate from the dry, super-cooled liquid crystalline phase. However, the situation is suggested to be even more complex. In the second heating cycle, there is also an exothermic peak at ca. 40 °C. This may indicate a relaxation or limited re-crystallisation process. Indeed, further evidence for the presence of transient crystalline or semi-crystalline states is obtained from PXRD data, as will be described below. If the same DSC experiment is conducted in a sealed pan, the same transitions are (somewhat surprisingly) observed, although the temperature and enthalpy of crystallisation are somewhat lower (Fig. 6, Table 2). The fact that the second heating cycle does not contain any melting of the hydrate (at 49 °C), in combination with the evidence for relaxation and/or re-crystallisation, suggest the system to be far from equilibrium and under kinetic control on the time scale of a DSC experiment. According to this line of reasoning, the crystallisation of the anhydrate is appreciably faster than that of the hydrate and there is no appreciable formation of the latter modification on the relevant time scale.

Before discussing the results obtained by SAXS, PXRD and polarised microscopy at elevated temperatures it must again be emphasised that all of the experimental set-up for these techniques allows for water to escape during measurement. Water may escape through the seals of the SAXS sample cell during measurement, particularly since the cell is housed in vacuum. Similarly, the PXRD and microscopy experiments were conducted in a manner where water can escape during heating of the sample. This means that the results from these three methods must be compared with DSC data recorded with open pans.

SAXS data show that when the endothermic transition at 49 °C is passed, the group of reflections at ca. 25 Å is shifted to distances with larger inter-lamellar spacing, where 38 Å is the dominating spacing based on the relative intensity (Table 1). In PXRD, a less well-defined diffractogram is obtained after having passed the transition, but the data are still consistent with a predominantly crystalline character (Fig. 7). However, the diffraction pattern is not attributable to the original material, nor is it attributable to the crystalline anhydrate obtained from freeze-drying. In addition, the position and intensity of the Bragg peaks change with time and temperature. The combined SAXS and WAXS data are thus fully compatible with a rapid solid–solid transition from a hydrated to a dehydrated modification at ca. 50 °C. However, the data also suggest that this transition proceeds via transient crystalline or semi-crystalline states. This agrees with the DSC data from the temperature-cycling experiments, where evidence for relaxation and re-crystallisation is observed (see above). When passing the endothermic event at 80 °C, all high-angle Bragg reflections are lost, confirming the formation of a liquid crystalline phase (Fig. 7).

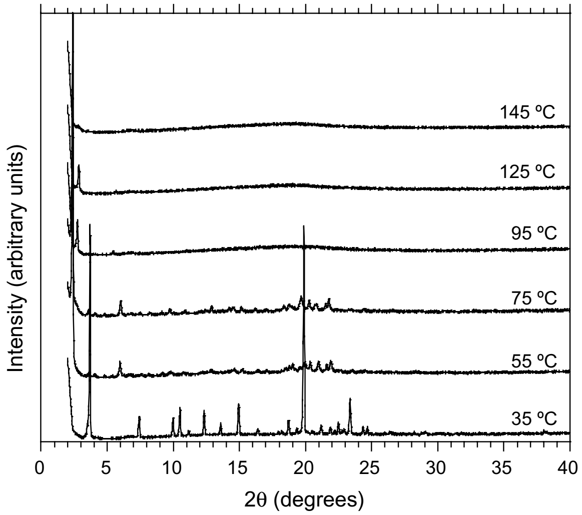

**Figure 7.** Powder X-ray diffractograms at different temperatures for β-$C_{12}G_1$ precipitated from water.

The thermotropic behaviour of the material was also studied with polarising microscopy in such a way that the temperature conditions of the DSC experiments conducted in open pans were simulated. No changes in optical properties were observed when passing the transition at 49 °C, but the chain melting at 80 °C gave rise to profound changes and was evident as a very rapid melting. Similarly, the transition from the liquid crystal to isotropic melt at the clearing point was easily detected due to the isotropic character and consequent black appearance in the microscope. Both exothermic peaks observed in DSC experiments upon decreasing temperature correspond to visible occurrences in the polarisation microscope. At the first exothermic transition (143 °C), Maltese crosses (typical for lamellar liquid crystals) were formed, and during further cooling they stayed roughly the same down to 47 °C. At this temperature they started to grow dramatically and develop into a richly coloured texture, indicative of a very rapid crystallisation process. The rate of the crystallisation lends support to the idea that the system is under kinetic control during DSC experiments.

The inter-lamellar distances observed for the hydrate (ca. 25 Å) is considerably smaller than that of the anhydrate (37 Å) and therefore suggest that the two structures comprise different chain-packing motifs. Again assuming an alkyl chain length of 16.7 Å and an extended glucoside head-group with a length of 5 Å,[26] a distance of ca. 25 Å is indicative of lamellar structures in which the alkyl chains are both interdigitated and tilted with respect to the bilayer plane. However, Goodby has suggested a lamellar structure in which the carbohydrate moieties from two adjacent layers overlap to produce an interdigitated hydrogen-bonded structure.[16] It would seem as if such a hypothetical structure would make it necessary for also the alkyl chains to be interdigitated in order to minimise the void. This, in turn, would lead to very small bilayer spacing, and the most realistic assumption for the hydrate seems to be that it contains interdigitated alkyl chains and non-interdigitated head-groups.

## 4. Conclusions

In the present work, a hydrate and an anhydrate of β-$C_{12}G_1$ have been characterised. Upon heating, the hydrate readily converts to the anhydrate, via transient crystalline states. This process seems to explain some previous inconsistencies in the literature. X-ray data strongly suggest that the chain packing in the anhydrate is different from that in the hydrate. More specifically, the alkyl chains in the hydrate are suggested to be interdigitated, whereas those in the anhydrate are not. For the liquid crystalline state, the lamellar spacing suggests a non-interdigitated chain packing.

Lyophilisation of β-$G_{12}G_1$ produces a crystalline anhydrate, rather than a glass or a super-cooled liquid crystalline phase. In contrast, lyophilisation of β-$C_{12}G_2$ and β-$C_{12}G_3$ produces glasses that may be regarded as 'frozen' versions of the corresponding lamellar liquid crystalline phase. For β-$C_{12}G_2$, the lamellar spacing is consistent with interdigitated alkyl chains in the glass and liquid crystal.

## Acknowledgements

This research has been funded by the Centre of Competence for Surfactants Based on Natural Products (SNAP) and AstraZeneca R&D Lund. Thomas Larsson is acknowledged for assistance during PXRD measurements and Dr. Lars-Erik Briggner for assistance and fruitful discussions about the PXRD, GVS, TGA and SS-DSC experiments.

## References

1. Auvray, X.; Petipas, C.; Dupuy, C.; Louvet, S.; Anthore, R.; Rico-Lattes, I.; Lattes, A. *Eur. Phys. J. E* **2001**, *4*, 489–504.
2. von Minden, H. M.; Brandenburg, K.; Seydel, U.; Koch, M. H. J.; Garamus, V. M.; Willumeit, R.; Vill, V. *Chem. Phys. Lipids* **2000**, *106*, 157–179.
3. Adasch, V.; Hoffmann, B.; Milius, W.; Platz, G.; Voss, G. *Carbohydr. Res.* **1998**, *314*, 177–187.
4. Vill, V.; von Minden, H. M.; Koch, M. H. J.; Seydel, U.; Brandenburg, K. *Chem. Phys. Lipids* **2000**, *104*, 75–91.
5. Jeffrey, G. A.; Bhattacharjee, S. *Carbohydr. Res.* **1983**, *115*, 53–58.
6. Jeffrey, G. A.; Yeon, Y.; Abola, J. *Carbohydr. Res.* **1987**, *169*, 1–11.
7. Bonicelli, M. G.; Ceccaroni, G. F.; La Mesa, C. *Colloid Polym. Sci.* **1998**, *276*, 109–116.
8. Kocherbitov, V.; Söderman, O. *Phys. Chem. Chem. Phys.* **2003**, *5*, 5262–5270.
9. Moews, P. C.; Knox, J. R. *J. Am. Chem. Soc.* **1976**, *98*, 6628–6633.
10. Dorset, D. L. *Carbohydr. Res.* **1990**, *206*, 193–205.
11. Hoffmann, B.; Milius, W.; Voss, G.; Wunschel, M.; van Smaalen, S.; Diele, S.; Platz, G. *Carbohydr. Res.* **2000**, *323*, 192–201.
12. Dorset, D. L.; Rosenbusch, J. P. *Chem. Phys. Lipids* **1981**, *29*, 299–307.
13. Balzer, D.; Lüders, H. *Nonionic Surfactants*; Marcel Dekker: New York, 2000.
14. Kocherbitov, V.; Söderman, O. *Langmuir* **2004**, *20*, 3056–3061.
15. Boyd, B. J.; Drummond, C. J.; Krodkiewska, I.; Grieser, F. *Langmuir* **2000**, *16*, 7359–7367.
16. Goodby, J. W. *Mol. Cryst. Liq. Cryst.* **1984**, *110*, 205–219.
17. Häntzschel, D.; Schulte, J.; Enders, S.; Quitzsch, K. *Phys. Chem. Chem. Phys.* **1999**, *1*, 895–904.
18. Verdonck, E.; Schaap, K.; Thomas, L. C. *Int. J. Pharm.* **1999**, *192*, 3–20.
19. Hyde, S. T. *Handbook of Applied and Colloidal Chemistry*; John Wiley & Sons: Chichester, 2002; Chapter 16, pp 299–332.
20. Laughlin, R. G. *The Aqueous Phase Behaviour of Surfactants*, 1st ed.; Academic: London, 1994.
21. Cecutti, C.; Focher, B.; Perly, B.; Zemb, T. *Langmuir* **1991**, *7*, 2580–2585.
22. Vill, V.; Böcker, T.; Thiem, J.; Fischer, F. *Liq. Cryst.* **1989**, *6*, 349–356.
23. Imamura, K.; Ogawa, T.; Sakiyama, T.; Nakanishi, K. *J. Pharm. Sci.* **2003**, *92*, 266–274.
24. Noel, T. R.; Parker, R.; Ring, S. G. *Carbohydr. Res.* **2000**, *329*, 839–845.
25. Boyd, B. J.; Drummond, C. J.; Krodkiewska, I.; Weerawardena, A.; Furlong, D. N.; Grieser, F. *Langmuir* **2001**, *17*, 6100–6107.
26. Nilsson, F.; Söderman, O.; Johansson, I. *Langmuir* **1996**, *12*, 902–908.
27. Ericsson, C. A.; Ericsson, L. C.; Kocherbitov, V.; Söderman, O.; Ulvenlund, S. *Phys. Chem. Chem. Phys.*, submitted for publication.